PROCEEDINGS OF SPIE

Omnidirectional optical transceiver design techniques for multi-frequency full duplex CubeSat data communication

Imam Uz Zaman, Andrew Janzen, Rasul Torun, Michael Y. Peng, Jose Velazco, et al.

SPIE.

Omnidirectional optical transceiver design techniques for multi-frequency full duplex CubeSat data communication

Imam Uz Zaman[*a], Andrew Janzen[b], Rasul Torun[a], Michael Y. Peng[b], Jose Velazco[b], Ozdal Boyraz[a]

[a]Electrical Engineering and Computer Science Dept., University of California, Irvine, USA 92617;
[b]Jet Propulsion Laboratory, NASA, Pasadena, CA, USA 91109

ABSTRACT

High speed (≥1Ghz) and long distance (≥100km) data communication among CubeSats and NanoSats can accelerate the technology advancement and paves the way for critical applications such as formation flying and remote sensing. Design of a simple, lightweight optical transceiver with full duplex capability, fast-tracking speed and 360º field of regard for CubeSat is crucial due to extreme SWaP-C limitations. In this paper, we describe the design tradeoff between the field of view and collection efficiency in receiver design using Commercial off the Shelf (COTS) optics and detectors. We also briefly discussed the design tradeoffs in transmitter design for optimum performance. We show that to achieve maximum SNR at long distance(≥100km), the laser beam diameter needs to be 80%-90% of the scanning mirror diameter. In addition to that, we show that the intrinsic Field of View (FOV) of high speed(≥600MHz) Avalanche Photodiodes (APD) can be increased to $\geq 3^o$ by incorporating optimized optics considering form factor of the CubeSat system. In addition, we present a scalable detector array design method using COTS components to achieve a wide full FOV(≥12º) with a uniform collection efficiency around 30%-60%. Furthermore, we demonstrated a multi-wavelength full duplex communication system based on dichroic filters as duplexer that shows significantly low crosstalk. The system also exhibits low transmission power loss(≤4%) as opposed to around 40% that of the conventional beam splitter based system.

Keywords: CubeSat, Omnidirectional, Optical Transceiver, Inter-Satellite, Optical Communication, Wide Field of View

1. INTRODUCTION

CubeSat and NanoSat technology continue to develop, and more sophisticated missions are being proposed and executed each year. In particular, recent CubeSat programs shows remarkable advancement in remote sensing applications[1–3]. Optical communication system allowing communication between multiple CubeSats is a potential favorite candidate for data relay and formation flying programs. Therefore, it can improve the sensing resolution and computational power in remote sensing applications. NASA's new mission for small spacecraft technology mandates small, affordable and transformative approaches to enable high-speed data communication and relative navigation without sacrificing performance metrics. Future CubeSats should be able to form a constellation, perform formation flying, and provide high-speed omnidirectional (>1Gbps) data communication and data relaying among satellites to share remote sensing data as in Figure 1. Indeed mass, volume, available power, pointing and acquisition accuracy, Signal to Noise Ratio (SNR) are important factors in the CubeSat design. Designing of a miniature optical transceiver is crucial in achieving omnidirectional communication capabilities. This paper describes design techniques and tradeoffs of CubeSat scale optical transmitter and receiver considering design constraints and component availability.
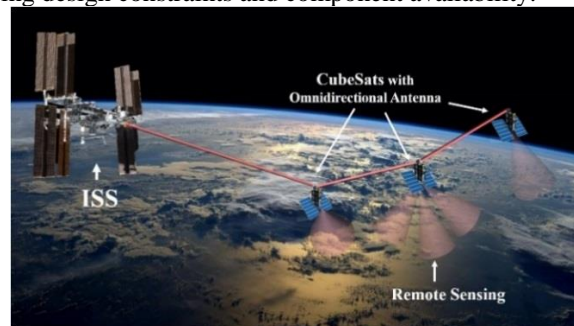
Figure 1. CubeSats with Omnidirectional Antennas in Formation Flying. A constellation can perform much complex and sophisticated task which requires more power and data processing capabilities than that of a single CubeSat.

*zamani@uci.edu

2. CUBESAT SCALE TRANSMITTER DESIGN TRADEOFFS

To achieve omnidirectional transmission, the compact transmitter needs to be designed according to the design tradeoffs among scanning mirror size, scanning angle, transmit beam width, beam divergence, pointing accuracy requirements in transmitter design to achieve high SNR($\geq$10dB) in high speed ($\approx$1Gb/s) communication. In the transmitter design techniques, it is very common to assemble the scanning mirror at 45° with respect to the incident laser beam axis. The optical path of the laser beam can support multiple large fixed mirrors without compromising the performance of the system and hence, the scanning mirror can be a limiting factor in designing the transmitter. Moreover, scanning capability of a mirror intertwined with its size, form factor, and driving mechanism. Full divergence angle (θ) of a Gaussian beam in free space is inversely proportional to its initial beam waist (ω_o) and proportional to the wavelength (λ) as in (1)[4]. As a result, a large initial beam exhibit less divergence as in (1) and therefore, facilitates higher the optical antenna gain.

$$\theta = \frac{4\lambda}{2\pi\omega_0} \tag{1}$$

Although incorporating a beam expander after scanning mirror is the easiest way to achieve larger beam waist than scanning mirror size, beam expander system decreases achievable scanning range. If M is the beam expansion ratio, then the system's scanning range (α) can be expressed as (2), where ϕ_m is the intrinsic scanning range of the scanning mirror.

$$\alpha \approx \frac{1}{M}\phi_m \tag{2}$$

In many cases, the scanning mirror diameter limits the allowable transmitter aperture where sacrificing scanning range is disadvantageous. Therefore, initial beam size needs to be optimized considering available scanning mirror parameters(size, speed, frequency) and far-field beam profile requirements. Relative size between the transmit beam and scanning mirror plays important role in optimizing far-field beam profile, beam size, scanning resolution, and peak intensity[5]. The collimated laser beam size (D_T) can be optimized to under-fill or over-fill the scanning mirror. A transmitted beam larger than the scanning mirror diameter (D_S) shows a smaller beam size at long distance ($\approx$100km) as in figure 2. Simulations show that far field beam radius decreases from $\approx$110m to $\approx$20m for a 5.5mm beam as the ratio, R=D_T/D_S increases from 20% to 90%. Moreover, it can be seen that the peak irradiance also increases up to a certain R and reaches at a maximum when 80%$\leq$ R $\leq$ 90% as shown in the figure. On the contrary, the beam profile gets distorted significantly due to different phenomena at the scanning mirror such as diffraction, scattering, beam clipping etc. when the beam size is comparable to mirror size. Figure 2 shows the distortion of beam profile with the increase of R. Three commercially available compact scanning mirrors (15mm, 10mm, and 5.5mm) are considered in far field beam size and irradiance simulation. Most of the scanning mirrors are procured from Mirrorcle Technologies[6] and Optotune[7]. Divergence data of all collimators are obtained from the datasheets of commercially available collimators[8–10] and hence, considered the non-ideal effects of actual optics inside collimators to achieve more realistic results from Zemax simulations.
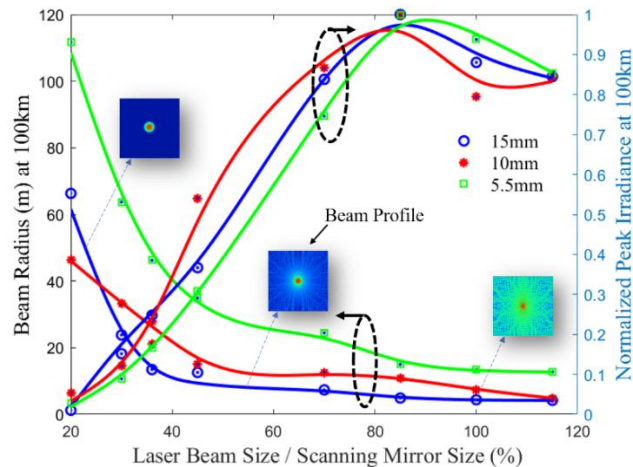
Figure 2. Effect of initial beam size to scanning mirror size ratio on far field beam size and peak irradiance. Three fast gimbal-less mirrors (15mm, 10mm, and 5.5mm) are considered in the simulation. The solid lines are fitted curve on the ZEMAX simulated data points based on COTS components.

3. CUBESAT SCALE OMNIDIRECTIONAL RECEIVER DESIGN

3.1 Receiver design techniques and tradeoffs

Compact, wide field of view multiple receivers need to be mounted inside the Cube to enable gimballess omnidirectional data communication. Depending on the geometry of the transmitter, the required full FOV of the individual receiver in a multi-receiver system can be in the range of 20°-65° to achieve omnidirectionality, which leads to challenging optical system design. In addition to wide FOV, the minimum optical power required by most COTS high speed (data rates ≥1Gbps) APDs are ≈ 6μW and ≈ 2μW for M=10 and M=100 relatively considering the required SNR of ≥13dB. Therefore, the receiver design techniques should consider the tradeoffs between FOV, detector bandwidth and power collection capability of the optics. Omnidirectional receiver design can be classified into two broader categories, Imaging Optics based Receiver (IOR) and Non-imaging Optics based Receiver (NOR). NOR[11–13] are highly used in solar cells to increase their efficiency by increasing their FOV. NOR possesses a tradeoff between optical power collection efficiency, aperture, size and achievable FOV. The simulation shows that, to achieve FOV>10 degrees with an aperture diameter of around 15mm, the required length of the conic structure, compound parabolic concentrator as well as compound elliptical concentrator is beyond CubeSat dimension (>20cm). As a result, we concluded that non-imaging-based receiver design is not a viable candidate for CubeSat scale wide FOV (≥30°) receiver design. On the other hand, the simplest IOR can be designed using an aspheric lens along with an Avalanche Photo Diode. However, detector's FOV depends on the diameter of the detector and the optics assembled with it as shown in (3)[14]. Here, H and F represents the detector diameter and focal length of the receiver lens. Equation 3 implies that it is desirable to use a large diameter detector to achieve wider FOV. However, detectors diameter is inversely proportional to its bandwidth (B) and hence, possesses design tradeoff.

$$FOV = 2 \times \tan^{-1}(\frac{H}{2F}) \tag{3}$$

In reality, large bandwidth (≥ 600MHz) commercial off the shelf APDs have diameters ≤1mm. Particularly 0.5mm and 1mm are the most available APDs as of today[15,16] which have bandwidth ≥ 600MHz. As a result, the receiver lens's focal length, F needs to be selected to get the desired FOV in designing high speed (≥1Gbps) receiver. It is known that, F ∝ diameter (D) and received power, $P_{rcv} \propto D^2$. Therefore, a lens with small F requires small D as well and therefore, decreases achievable optical power. Consequently, the attainable communication link SNR and communication distance declines. One way to increase the FOV of the detector is to utilize a ball lens at the focal point of the receiver lens as shown in Figure 3. For example, a detector system incorporating 25mm diameter and 30mm focal length can achieve FOV of approximately ±0.5° (efficiency ≥50%) if no ball lens is used (Figure 3). However, the simulation shows that the FOV can be doubled (±1° approx.) utilizing half-ball lens of 4mm diameter. Further FOV improvement can be achieved by using a larger detector. For example, 1mm detector along with 2mm ball lens can achieve ±1.6° FOV. To achieve omnidirectionality, we need quite a lot of this receiver system to achieve 360° FOV. Therefore, this simple system is not feasible for omnidirectional CubeSat system.
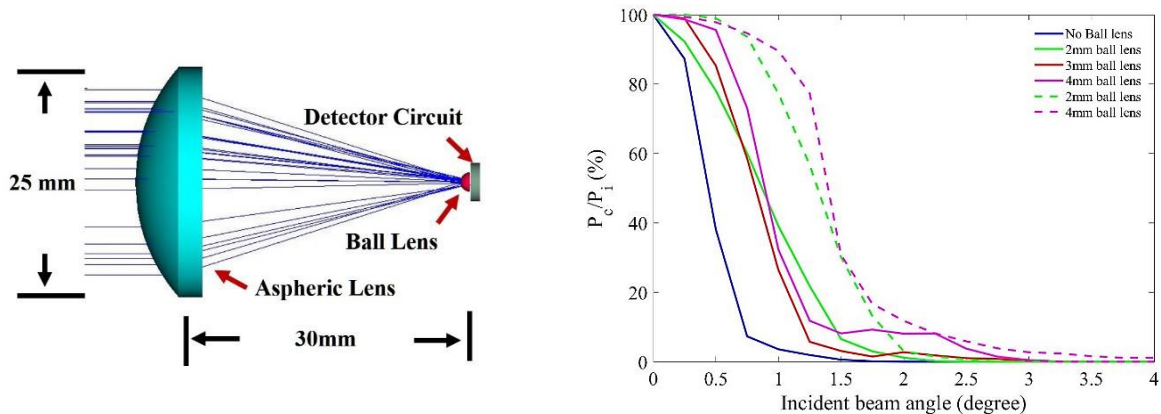
Figure 3. (Left) Simplest IOR using an aspheric lens, a ball lens and a detector. (Right) Detector collection efficiency of the system with incident beam angle. Pc and Pi are the collected power at the detector and the power received by the receiver lens. The solid and dashed lines represent 0.5mm and 1mm detectors respectively.

A second IOR can be designed by adopting a Fish Eye Lens (FEL) system. Surely, FEL[17] can achieve very high FOV ($\approx$ 180°)[18], nevertheless, the received optical power and therefore, SNR for a certain solid angle is significantly low. As a result, FEL is not advisable for high speed, long distance data communication. Another alternative is to use a Detector Array (DA). A scalable, small form factor detector array incorporating APD dies, ball lens and an aperture can achieve a collection efficiency of $\approx$40% and FOV$\geq$12°. Detail analysis on such DA is described in the following section.

3.2 Scalable detector array

A compact detector array (as shown in Figure 4) is a feasible way to achieve very wide FOV. The DA in Figure 4 consists of 27 Detector Units (DUs). The design requires compact, bezel less, high speed (>1Gbps) detectors to attain uniform light collection. For example, DU, as in figure 4(a) is designed based on the spec of a commercial APD die ($\approx$0.5mm), a 1.5mm ball lens and a custom designed miniature APD Chip. This DUs can be arranged to achieve a scalable Detector Array (DA) of any size and shape. An example of compact array for CubeSat application is shown in Figure 4(b). An aspheric lens aperture is used to increase the detected power and hence, to improve SNR in long distance ($\geq$100km) communication.
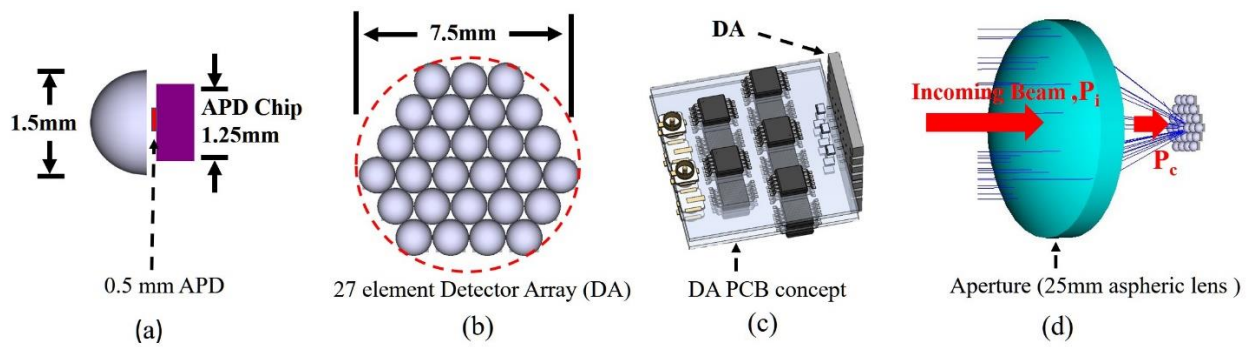
Figure 4. (a) DU made up of a small ball lens, an APD die and an APD circuit, (b) Detector array consist of 27 DU in a $\approx$7.5mm diameter circle, (c) DA printed circuit board concept, (d) A 25mm aspheric lens aperture to increase collection power.

As might be expected, the development of scalable DA possesses some design challenges and performance limitations. First, DA's collection efficiency (P_c / P_i), where P_i and P_c are the optical power incident at the aperture and optical power collected by the detector array, varies with the incident beam angle due to the form factor of the detector size and other optics. Second, the electric circuit design complexity increases with the scaling of the array as shown in Figure 4(c). Third, collection efficiency uniformity over a FOV depends on a number of detectors to integrate. Fourth, summing up the signals from selected detectors for a particular angle requires an advanced algorithm and owns the possibility to accumulate noise. Last of all, multiple DAs with a mechanical rotation system are required to achieve omnidirectional data communication and relaying, which brings significant mechanical design complication.

Figure 5 shows the collection efficiency for different DA placement relative to aperture lens focal plane for both X-axis incident angle (θ_X) variation (left) and Y-axis incident angle (θ_Y) variation (right). It is evident from figure 5 that ball lens increases individual detectors' FOV (the solid green line is wider than the dashed blue line). The mean collection efficiency with ball lens system is 57%, that is around 24% higher than the system without ball lens when that the DA is positioned at 0 mm relative distance from Focal Plane (FP) (Table 1). As a result, the collection efficiency is significantly higher in the presence of ball lens. For example, assuming that the DA is placed 3mm further from FP, that mean collection efficiency is 37% with ball lens and 10% without ball lens. It can be seen that the placement of the DA is important to achieve desired performance. Placement of the DA at the FP of aperture lens decreases collection efficiency uniformity due to form factor of DA. It can be seen from Figure 5, that inspite of attaining maximum ($\approx$98%) collection efficiency at some discrete angle, the collection efficiency curve shows periodic dips if the DA is placed right at the FP of the aperture lens. Indeed, this system shows a very high standard deviation of around 41%. Consequently, this DA placement is not suitable for dynamic communication system, where two communication nodes are continuously changing positions as in inter-satellite communications.
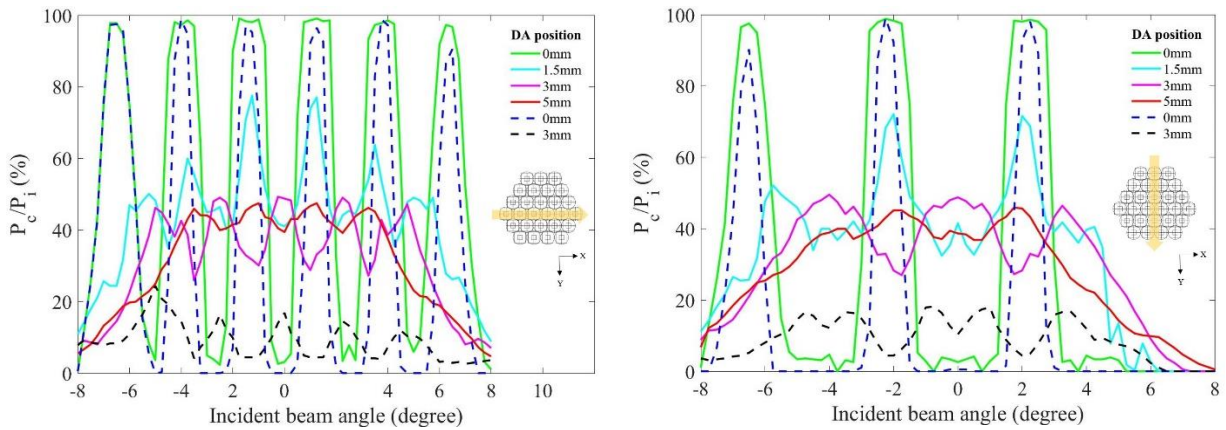
Figure 5. The collection efficiency of DA with incident angle variation along X axis (left) and along Y axis (right). The solid lines and dashed lines represent DA system with mounted ball lens and without ball lens respectively.

On the contrary, significant collection uniformity can be achieved by placing the DA little bit further from the focal plane. For instance, by placing DA 3mm further from FP, a mean collection efficiency, $\mu =37\%$ with standard deviation, $\sigma= 11\%$ is achievable over a $\pm 6^{\circ}$ incident angle variation along Y axis as in Figure 5 (right) and $\mu=37\%$ with $\sigma=8\%$ is achievable along X axis as seen in Figure 5 (left). Table 1 summarizes the collection efficiency data for all angular variation and DA placement.

Table 1. The collection efficiency of the detector array.

Incident angle	$-6^{\circ} \le \theta_X \le 6^{\circ}$						$-7^{\circ} \le \theta_Y \le 5^{\circ}$					
Mounted ball lens	✓	✓	✓	✓	x	x	✓	✓	✓	✓	x	x
DA position w.r.t FP (mm)	0	1.5	3	5	0	3	0	1.5	3	5	0	3
μ (rounded) in %	57	49	37	36	33	10	30	40	37	34	15	11
σ (rounded) in %	41	10	8	9	40	5	41	14	11	10	34	5

It is evident from the abovementioned discussion that by the Optimum design of detector array a very wide full field of view (>12°) is achievable. This DA can achieve required SNR to achieve high-speed data communication. Deciding the number of detectors to integrate in achieving uniform collection efficiency over a particular collection angle is crucial in designing detector array. In the above-mentioned simulation, we assumed integration block is composed of closely located 1, 3, 5, 6 detectors for DA position of 0mm, 1.5mm, 3mm and 5 mm from the aperture lens's focal plane accordingly. Admittedly, the electronics design and signal analysis complexity increase with the number of detectors in integration block and limit design flexibility. Therefore, in the simulation, the number of detectors in the integration block are chosen considering the design feasibility. Nevertheless, with optimum design of DA decision circuits and sophisticated post signal processing, this scalable detector array can achieve fast data rate and very wide FOV in numerous free space communication systems.

4. A LOW LOSS FULL DUPLEX TRANSCEIVER DESIGN SCHEME

A full duplex, compact transceiver design can overcome the receiver design challenges and tradeoffs as mentioned in the previous section. In a Full Duplex Transceiver (FDT) the same aperture is used to transmit and receive the signal. As a result, communicating CubeSats will always be at the direct line of sight under the assumption that the Pointing, Acquisition and Tracking (PAT) system can detect the Angle of Arrival with good precision. In such FDT design, a COTS beam splitter is a candidate to be used as a duplexer. However, the beam splitter inherits some performance limitations. First, it reduces the transmission power as well as received optical power by around 30%-50% due to beam splitting and hence, limits the achievable communication distance. Second, the back reflection, cross talk and scattering from beam splitter is high, which result in low receiver sensitivity. Third, beam splitter is relatively heavier, and as a result, using

multiple beam splitters in weight limited system is provocative. The abovementioned drawbacks make beam splitter unalluring for omnidirectional CubeSat receiver design. On the other hand, a transceiver design with a dichroic filter as a duplexer shows promising result. We designed a multi frequency full duplex transceiver as in Figure 6. The aperture (transmitter and receiver) is a dual axis vector scanning mirror (15mm diameter) with ±25º mechanical scanning ability. The scanning ability of the aperture ensures point to point, line of sight communication link among communication nodes in any circumstances. Figure 6 shows the experimental setup of one side of the FDT. All components are chosen considering CubeSat's size, power and space limitation. In reality, 5 of the FDTs (except 8, 9) can be fit inside 1U to achieve omnidirectional FOV.
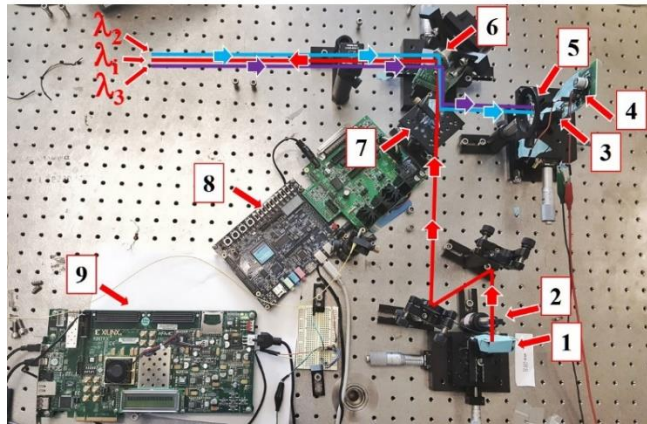
Figure 6. One side of the experimental setup of full duplex multi frequency transceivers. 1- 880nm laser, 2- collimation lens, 3- APD, 4- APD circuit board, 5- focusing lens, 6- scanning mirror, 7- 850nm long pass dichroic filter, 8, 9- FPGA boards to control the system. The other side of the communication link is identical except an 808nm laser and an 850 short pass filter are used.

To minimize the cross talk at the receiver, we plan to assign a slightly different wavelength (λ_i) to each CubeSat (C_i) in a constellation of n CubeSats. The dichroic mirror (m_i) for a C_i is selected in such a way that it allows only λ_i to pass and reflect other wavelengths as shown in Figure 6. This multi-wavelength system design reduces the power loss in both transmission and receiving channels. Moreover, measurement shows notable reduction in cross talk due to dichroic filter. To prove the concept, we choose two lasers of 808nm and 880nm, an 850nm short pass dichroic filter and an 850nm long pass filter. Figure 7 shows the block diagram of the experimental setup and data points. In addition to that, Table 2 summarizes the experimental DC measurements of the preliminary system.
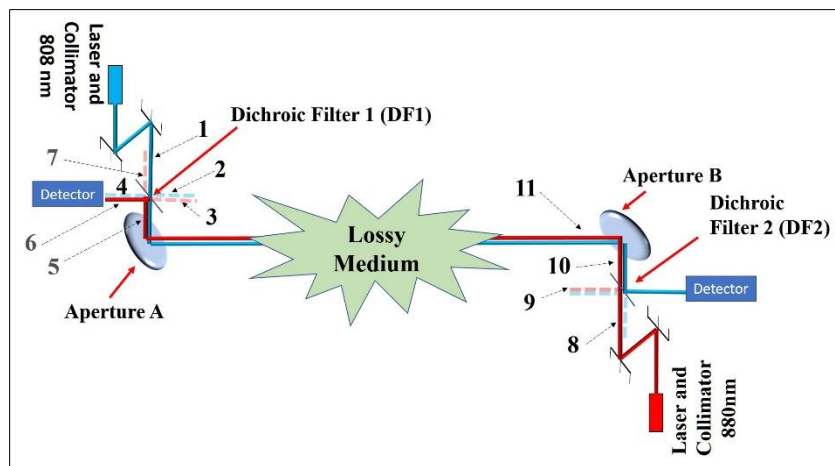
Figure 7. Block diagram two frequency Full Duplex Transceiver (FDT) experimental setup. The numbers represent measurement points. The left and right transceivers are named as transceiver A and transceiver B in Table 2.

Experimental data (Table 2) shows a non-discernable (below detector noise) crosstalk (4 in figure 8) caused by duplexer, in our case dichroic filters. Moreover, transmission power loss due to dichroic filter is around 2% - 4% depends on the coating quality and wavelength. Which is still significantly higher than that of beam splitter-based system (30%-50%). Low crosstalk and low transmission loss are the main advantages of multi-wavelength (multi-frequency) based system. Although, experiment is conducted at 800nm – 900nm wavelength region, the multi frequency FDT system is feasible at telecom wavelength. The system is also scalable to build a local communication network incorporating a large number of CubeSats by choosing a closely spaced wavelengths and matched DFs. However, we acknowledge that the scalability of the system largely depends on available COTS dichroic mirrors. Although a few dichroic filters (45° AOI) is commercially available, customized DFs can be obtained from different research labs. Further research will involve frequency domain measurements, BER estimation, and detector noise calculation extensively.

Table 2. Experimental Data from the setup as in Figure 7.

	Transceiver A			Transceiver B	
Point	Description	Measured power (mW)	Point	Description	Measured power (mW)
1	808nm laser output	10.4	8	880nm laser output	10.3
2	Power loss at DF1	0.303	9	Power loss at DF2	0.245
3	Transmit power (808nm)	10.01	10	Transmitter power(880nm)	10.1
4	Crosstalk component	N/A	11	Power after steering mirror	9.7
5	Received Power (850nm)	5.3		Transmission of DF1= 96%	
6	Power at APD	5.218		Transmission of DF2=98%	
7	Received Power loss at DF	0.082		Measurement error < ±3%	

5. CONCLUSION

In this paper, we discussed the design tradeoffs of different receiver design approaches considering SWaP-C limitation imposed by the CubeSat parameters. We also briefly discussed transmitter design tradeoffs in achieving compact, omnidirectional antenna. Moreover, we showed the caveats (size, FOV, power collection) of conventional receiver design approaches such as non-imaging optics, simple imaging receiver, fish eye lens etc. to adopt in CubeSat scale design. We showed that by optimizing the ball lens and aspheric lens, a simple receiver design can achieve ≈3.2° full FOV. Furthermore, we presented design concept of a compact scalable detector array that can obtain a FOV ≥10°. A dichroic mirror based multi wavelength Full Duplex Transceiver system is also presented. Preliminary data of the low power loss (≈3%) and low crosstalk (≈0) validates the feasibility of this FTD design approach in achieving omnidirectional optical communication.

6. ACKNOWLEDGEMENT

REFERENCES

[1] Mahmoud, A. A., Elazhary, T. T. and Zaki, A., "Remote sensing CubeSat," Sensors, Systems, and Next-Generation Satellites XIV **7826**, 78262I, International Society for Optics and Photonics (2010).
[2] Peral, E., Im, E., Wye, L., Lee, S., Tanelli, S., Rahmat-Samii, Y., Horst, S., Hoffman, J., Yun, S. H., Imken, T. and Hawkins, D., "Radar Technologies for Earth Remote Sensing From CubeSat Platforms," Proceedings of the IEEE **106**(3), 404–418 (2018).

[3] Qiao, L., Glennon, E., Dempster, A. G. and Chaoui, S., "Using cubesats as platforms for remote sensing with satellite navigation signals," 2013 IEEE International Geoscience and Remote Sensing Symposium - IGARSS, 852–855 (2013).

[4] Anthony E. Siegman., [LASERS], 665–672.

[5] Imam Uz Zaman, Andrew W. Janzen, Rasul Torun, Michael Peng, Jose E. Velazco and Ozdal Boyraz., "Design Tradeoffs and Challenges of Omnidirectional Optical Antenna for High Speed, Long Range Inter CubeSat Data Communication," Small Satellite Conference, Delivering Mission Success, SSC18-WKII-06 (2018).

[6] Technologies, M., "Mirrorcle Technologies MEMS Mirrors - Technical Overview."

[7] "Optotune.", <https://www.optotune.com/>.

[8] Micro Laser System Inc., "Adjustable Fiber Collimators," <http://www.microlaser.com/FiberOptic/FiberCollimators.html>.

[9] Thorlabs., "Collimation / Coupling," <https://www.thorlabs.com/navigation.cfm?guide_id=27>.

[10] Princetel., "FIBER COMPONENTS: Large-beam fiber collimators," <http://www.princetel.com/fc_clx.asp>.

[11] Broman, L., "Non-Imaging Solar Concentrators With Flat Mirrors," Intl Conf on Nonimaging Concentrators **0441**, 102–110, International Society for Optics and Photonics (1984).

[12] Ries, H. and Rabl, A., "Edge-ray principle of nonimaging optics," J. Opt. Soc. Am. A, JOSAA **11**(10), 2627–2632 (1994).

[13] Miñano, J. C. and González, J. C., "New method of design of nonimaging concentrators," Appl Opt **31**(16), 3051–3060 (1992).

[14] "Understanding Focal Length and Field of View.", <https://www.edmundoptics.com/resources/application-notes/imaging/understanding-focal-length-and-field-of-view/>.

[15] "Low bias operation, for 800 nm band.", <https://www.hamamatsu.com/jp/en/product/type/S12023-10/index.html>.

[16] "Marktech Optoelectronics.", <https://www.marktechopto.com/>.

[17] Deng, P., Yuan, X., Zhao, M., Zeng, Y. and Kavehrad, M., "Off-axis catadioptric fisheye wide field-of-view optical receiver for free space optical communications," OE, OPEGAR **51**(6), 063002 (2012).

[18] Kumler, J. J. and Bauer, M. L., "Fish-eye lens designs and their relative performance," Current Developments in Lens Design and Optical Systems Engineering **4093**, 360–370, International Society for Optics and Photonics (2000).